



# A SERS nano-tag-based fiber-optic strategy for *in situ* immunoassay in unprocessed whole blood

Xiaokun Li<sup>a,b</sup>, Youlin Zhang<sup>a,\*</sup>, Bin Xue<sup>a</sup>, Xiangui Kong<sup>a,\*</sup>, Xiaomin Liu<sup>a</sup>, Langping Tu<sup>a</sup>, Yulei Chang<sup>a</sup>, Hong Zhang<sup>c,\*</sup>

<sup>a</sup> State Key Laboratory of Luminescence and Applications, Changchun Institute of Optics, Fine Mechanics and Physics, Chinese Academy of Sciences, 130033 Changchun, China

<sup>b</sup> State Key Laboratory of Electroanalytical Chemistry, Changchun Institute of Applied Chemistry, Chinese Academy of Sciences, 130033 Changchun, China

<sup>c</sup> Van't Hoff Institute for Molecular Sciences, University of Amsterdam, Science Park 904, 1098 XH Amsterdam, The Netherlands

## ARTICLE INFO

### Keywords:

SERS nano-tags  
Silica encapsulation  
Fiber-optic biosensor  
Whole blood

## ABSTRACT

Assay technologies capable of detecting biomarker concentrations in unprocessed whole blood samples are fundamental for applications in medical diagnostics. SERS nano-tags integrated fiber-optic biosensor (FOB) was realized for the first time for *in situ* immunoassay in whole blood. The reliability and sensitivity of this method rely, in a large extent, on the quality and properties of the SERS nano-tags. The constructed silica-coated Ag SERS nano-tags as labels were used in a rapid and specific *in situ* FOB immune sensor to detect alpha fetoprotein (AFP) in unprocessed blood samples. Preliminary results of *in vivo* and *in situ* dynamic observation of AFP of whole blood in wistar rat highlight the power of this new method.

## 1. Introduction

The detection of the contents of blood composition can provide scientific basis for clinic diagnosis, prognosis, and prevention and control measure. Unfortunately, the relevant detections are mainly carried out in plasma or serum samples, separated from the whole blood, which require considerable sample preparation, making these assays expensive, time-consuming, complexity, less accurate. Worse, this requires that the tests are carried out in the central laboratories and precludes them from most point-of-care (POC) applications (Sun et al., 2013). Thus, for many POC and public health applications, it is very important to design practicable strategy to detect biomarker directly in unprocessed whole blood samples without introducing the complicated sample preparation.

Among the developed detection techniques, optical detection methods have been regarded as one of the most convenient tools due to the simplicity and low detection limit (Pansare et al., 2012; Wencel et al., 2014). However, the strong scattering, absorption, and significant autofluorescence from the whole blood limit their application in the whole blood (Arppe et al., 2015; Pansare et al., 2012; Xie et al., 2013). Some articles have reported homogeneous assay in the application of whole blood, the results of detection would hold many errors and the lower sensitivity because the light scattering effect has to be thought due to the complexity of whole blood compositions according

to the light scattering theory (Li et al., 2012; Wencel et al., 2014). The only manner to eliminate the light scattering effect is to avoid the light spread in the whole blood solution. Taking advantage of optical fiber, we introduce the optical fiber bio-sensing technology to eliminate the influence of light scattering effect (Zhang et al., 2010; Wang and Wolfbeis, 2013; Bosch et al., 2007; Leung et al., 2007). Where the function of optical fiber is to transmit the excitation light and signal, and the other function is used as the supporter of the indicators. Among one of them, fiber-optic bio-sensor (FOB) based on evanescent wave has great potential in POC application due to many advantages such as easy operation, no separation, higher sensitivity and the detection can be implemented *in situ*, real-time and *in vivo* (Taitt et al., 2005; Zhang et al., 2010). The evanescent wave from the fiber core can only excites the fluorophores in vicinity of fiber core within about 100 nm, partly avoiding the interference from the environment, bringing the above merits. However, in whole blood assay, the blood can still exist in the evanescent wave region. So, the direct application of this technology into whole blood sample maybe demands that both excitation and detection region lie in the near-infrared (NIR) window to avoid background interference, because the whole blood possesses strong background absorption and autofluorescence in UV–visible (UV–Vis) region (Arppe et al., 2015).

SERS nano-tags, as NIR probes, have gained widespread attention due to their exceptional photophysical properties (Sha et al., 2008;

\* Corresponding authors.

E-mail addresses: [zhangyl@ciomp.ac.cn](mailto:zhangyl@ciomp.ac.cn) (Y. Zhang), [xgkong14@ciomp.ac.cn](mailto:xgkong14@ciomp.ac.cn) (X. Kong), [h.zhang@uva.nl](mailto:h.zhang@uva.nl) (H. Zhang).

Wang et al., 2013). For example, compared to other tags, e.g. QDs, and dyes, SERS tags are superior in multiplexing, ultra-sensitivity, high-photostability, and quantitative abilities. Importantly, SERS nano-tags overcome the shortcomings of the other NIR probes, e.g. no photobleaching and the much more number of distinct signals in the NIR window. Therefore, SERS nano-tags are under more and more active investigation for *in vivo* applications. Moreover, SERS nano-tags have been also employed in homogeneous assay in unprocessed blood (Sha et al., 2008). Therefore, SERS nano-tags in combination with FOB has great potential to be used to develop a simple and *in situ* assay method in whole blood samples without the blood separation steps.

In this work, taking advantage of the intrinsic properties of the SERS nano-tags and FOB, we have developed a SERS nano-tag-based fiber-optic strategy to be successfully used for *in situ* immunoassay in the unprocessed whole blood that overcomes the current assay limitations. This method largely relies on the properties of SERS nano-tags. We have prepared silica-coated SERS nano-tags, comprised of one SERS-active Ag nanoparticle (NP) and a sub-monolayer of 4-MBA Raman molecules adsorbed to the Ag NP surface, and a silica shell to protect SERS nano-tags and further functionalization. The as-constructed Ag@4-MBA@SiO<sub>2</sub> nano-tags displayed stronger SERS signals with the enhancement factor of  $1.5 \times 10^7$  (AEF), and processed excellent stability in the unprocessed whole blood solutions. We further integrated these Ag@4-MBA@SiO<sub>2</sub> SERS tags with optical fiber to construct an *in situ* immune assay for direct measuring cancer biomarker, alpha-fetoprotein (AFP) in unprocessed whole blood solutions. The results demonstrated the constructed FOB in whole blood held sensitive and reproducible response to the AFP concentration in the range from 50 to 500 ng/mL. Preliminary results of *in vivo* and *in situ* dynamic observation of AFP of whole blood in wistar rat demonstrated this method had the great potential in *in vivo* assay. At the same time, the dynamic observation of AFP in PBS and unprocessed blood samples proved the complicated composition seriously influenced the diffusion coefficient.

## 2. Experimental section

### 2.1. Materials

Tetraethyl orthosilicate (TEOS, 98%), aminopropyltriethoxysilane (APTMS) and 4-mercaptobenzoic acid (4-MBA) were purchased from Sigma-Aldrich. Sodium citrate, dimethylamine, anhydrous isopropanol, NaBH<sub>4</sub> and NaCl were obtained from Beijing Chemical Plant. Silver nitrate (AgNO<sub>3</sub>, ≥99%) was purchased from Fluka. The whole blood was supplied by Changchun Blood Supply Center (Changchun, China). Alpha Fetoprotein antibody (Rabbit anti-AFP) and Alpha Fetoprotein (AFP) were purchased from Beijing Dingguo Biotechnology Company (Beijing, China). Deionized water was purified through a Milli-Q water purification system and the resistivity was 18.2 MΩ cm.

### 2.2. Encapsulating the SERS-Ag NPs with silica

SERS reporter-functionalized Ag NPs were further encapsulated with a silica shell based on our before article (Zhang et al., 2015). Simply, as-prepared SERS-functionalized Ag NPs solution (2 mL) was added into isopropanol (8 mL) solutions. Under shaking, dimethylamine solution (0.2 mL, 30 wt%) was added to the mixed solution, followed by the addition of TEOS in isopropanol (0.6 mL, 10 mM) three times within 6 h after 10 h, the reaction mixture was then centrifuged at 8500 rpm for 15 min and Ag@4MBA@SiO<sub>2</sub> NP precipitate was redispersed into ethanol for further washing. After three times of washing, Ag@4-MBA@SiO<sub>2</sub> NPs were obtained and redispersed into deionized water or ethanol (2 mL) for characterization and further functionalization.

### 2.3. Modification of Ag@4MBA@SiO<sub>2</sub> SERS nano-tags

2 μL of APTMS was added into the NPs anhydrous ethanol solution and stirred for 12 h (You et al., 2012). Then, the above solution was centrifuged three times by washing with ethanol. The obtained Ag@SiO<sub>2</sub> NPs were dropped into glutaraldehyde (GA) solution (1%). After 2 h, the Ag@SiO<sub>2</sub> NPs were centrifuged three times with water. The remnant was finally dissolved in 10 mM PBS buffer, and AFP was then added for protein immobilized on the surface of the tag NPs overnight and then dipped into 1% (m/m) albumin from bovine serum (BSA) solution for 2 h.

### 2.4. Preparation of rabbit anti-AFP functionalized fiber-optical ends and *in situ* assay in the whole blood

The cladding was firstly taken down from the lateral face of the optical fiber and buffered 12.5 cm from the distal end. To prepare rabbit anti-AFP -functionalized optical-fiber was based on our before article (Zhang et al., 2010). Simply, the optical fiber core was firstly cleaned to get rid of the contaminant and activate the hydroxyl. Then, the aldehyde-functionalized fiber probes were obtained by using the reagents: APTMS and GA. At last, the fiber probes were coated overnight with 1 mg/mL rabbit anti-AFP at 4 °C and then dipped into 1% (m/m) BSA solution for 2 h. The displacement immunoassay was prepared as follows. Firstly, rabbit anti-AFP modified fibers were added into AFP modified SERS tags solution for 4 h and then cleaned three times.

The FOB was applied to show the advantage of Ag@SiO<sub>2</sub> SERS tag as labels for rapid detection of the AFP in unprocessed whole blood solutions. A series of different concentration of AFP whole-blood solutions were prepared by adding different amount of AFP to 1 mL of whole blood. Then the fibers were dipped into the whole blood samples for 30 min to measure the SERS signals.

In a proof of concept experiment, the AFP was injected into the wistar rat by jugular. After 30 min, the fiber-optical probe was dipped into tail vein by using syringe needle and then measured the SERS signal in different moment in order to demonstrate an *in vivo*, *in situ* and real time assay concept.

### 2.5. Characterization

The size of NPs was measured by field emission scanning electron microscopy (FE-SEM, Hitachi, S-4800). The Raman spectra were measured at room temperature by an Ocean Optics QE65000 Raman spectrometer system equipped with a 785 nm laser. All the Raman measurements were completed in the solution.

### 2.6. Design of direct immunassay in unprocessed whole blood

As talked above, optics-based assay technology is not fit for detecting biomarker directly in whole blood, which is the main subject of strong background absorption in UV–Vis region, autofluorescence and light scattering from the whole blood components.

Here, we design a new strategy of SERS nano-tag integrated fiber-optic sensing strategy for *in situ* detecting biomarker in the unprocessed blood. The SERS nano-tags can be excited by using the NIR laser-785 nm, which clears up the background noise from the whole blood. Thinking about the advantages of the optical fiber, the optical fiber is introduced to eliminate the influence of light scattering from the blood components and even bring the other functions such as *in situ* and *in vivo* by using evanescent wave theory. The reliability and sensitivity of this strategy rely, in a large extent, on the quality and properties of the SERS nano-tags. “Bare” SERS nano-tags are instable and show biotoxicity to limit their applications. Encapsulation of silica on the SERS tags to form core-shell structure is used to overcome the above problems. Fig. 1 shows the basic steps for the unprocessed whole

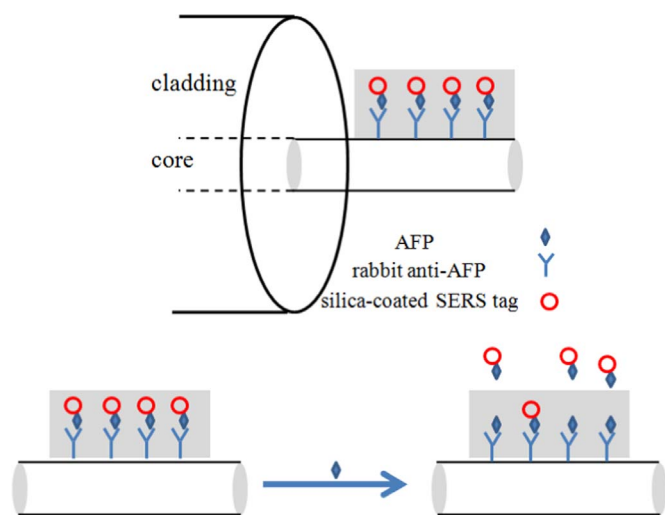


**Fig. 1.** Illustration of displacement assay using FOB. Gradient grayness indicates the exponentially decaying electric field of the evanescent wave.

blood assay. Alpha fetoprotein (AFP) is selected as an example. Gradient grayness in Fig. 1 indicates the exponentially decaying electric field of the evanescent wave, coming from the evanescent wave theory. The SERS nano-tags outside the gradient grayness region can not be excited. Therefore, this strategy can possess the function of *in situ* and *in vivo*.

### 3. Results and discussion

#### 3.1. Fabrication of SERS tags covered with an inert silica shell

SERS, which can detect even at a single molecule level, has great potential in bioassays (Nie and Emory, 1997). In the SERS tags, Ag cores provide a high electromagnetic field to amplify the Raman signal of reporter. Silica shell prevents the Raman reporter from leaching and the adsorption of the interfering molecules onto the metallic surfaces, and importantly, brings in high stability, good biocompatibility and ease of further modification for biological applications (Wang et al., 2013). The citrate-stabilized Ag NPs are suitable base for SERS tag because Raman molecules are easy to be adsorbed on the citrate-stabilized Ag NP surface. 4-MBA molecule was selected as Raman reporter, where the 4-MBA can be bound on the Ag NP by using the interaction between the thiol groups and Ag NP, due to the fixed spectral recognition and good Raman scattering cross (Bishnoi et al., 2006). The SERS tags were encapsulated by TEOS to produce the silica-coated SERS tags. The thickness of silica shell was controlled by repeatedly adding the TEOS into the reacting solution at a time interval of 2 h. Monodisperse Ag@4MBA@SiO<sub>2</sub> were successfully prepared via the modified Stöber method. The morphologies of the Ag and Ag@4MBA@SiO<sub>2</sub> were characterized with FE-SEM. The synthesized Ag NPs were nearly spherical with an average diameter of 25 nm (Fig. S1). The Ag@4MBA@SiO<sub>2</sub> NPs are nearly spherical and uniform, and their diameter increases with increasing TEOS amount (Fig. 2). The results show the silica shells are homogeneous with thickness of about 25 nm and the nano-spheres are highly monodisperse. The core/shell nanostructures are clearly seen due to the strong contrast between the white cores and gray shells, which provides direct evidence that the Ag NPs are completely encapsulated with silica shells. The thickness of the silica shells could be tuned by varying the amount of added TEOS (Zhang et al., 2015).

The signal intensity of the SERS tags is very necessary for the assay sensitivity. We now turned to the influence of silica-encapsulation on the SERS signal. Fig. 3 shows Raman spectra of silica-coated SERS tags and SERS tags before silica encapsulation. In Fig. 3, the SERS tags

display strong and unique spectroscopic signatures. Obviously, the peak positions remain unchanged upon the encapsulation, indicating that the silica coating does not vary the structure of Raman reporter. The signal intensities of 4-MBA slightly increase after silica encapsulation, verifying no apparent loss of 4-MBA during encapsulation due to the strong affinity to the Ag NP surface. The increase of intensities maybe comes from the increase of the refractive index due to silica (Kong et al., 2012). We have also estimated the SERS enhancement factor (AEF) by using the following relationship:  $EF = (I_{SERS} \times C_{NR}) / (I_{NR} \times C_{SERS})$ , where  $I_{SERS}$  and  $I_{NR}$  are the intensity of the bands for SERS and normal Raman scattering, respectively, and  $C_{NR}$  and  $C_{SERS}$  are the concentration of Raman molecules in pure solution and the Ag NP solution (Scarabelli et al., 2014). The peak intensity at 1076 cm<sup>-1</sup> (for 4-MBA) was used to estimate the AEF. The calculated AEF was about  $1.5 \times 10^7$ , demonstrating the constructed SERS tags possess the ability to sensitively detect the analyte.

As is well known, one of merits of silica-coating SERS is the long-term storage. Their stability depends on the silica shell thickness. It is therefore important to study the influence of silica shell thickness on the SERS signal. It was found that the SERS intensity began to decrease when the shell thickness was bigger than 30 nm, which was probably due to scattered increase and/or the influence of silica shell on laser focusing (Kong et al., 2012). So in this article, we use the silica-coated SERS tags showed in Fig. 2 as the labels.

#### 3.2. Raman measurement in unprocessed whole blood

To demonstrate the feasibility of the silica-coated SERS tags as labels used for the analysis of whole blood samples, the absorption spectra of the whole blood samples were examined. Fig. S2 shows the UV–Vis absorption spectra of the whole blood diluted by 40 fold. The spectrum of whole blood was too strong to obtain a reasonable spectrum, so the whole blood samples must be diluted to perform the UV–Vis measurement. There are two strong absorptive bands between 500 and 600 nm. No absorption is observed above 700 nm, implying optical measurement in whole blood samples is always interfered severely when the excitation wavelength is located in the UV–Vis region. For example, the evanescent wave-based optical fiber biosensor (FOB), as far as possible, reduces the interference from the surrounded environment by using the evanescent wave theory. However, the evanescent wave-based FOB with the QDs as labels (Zhang et al., 2010) was used to directly detect the whole blood samples, the interference from the whole blood could not be avoid. As shown in Fig. S3, strong background signal from the whole blood was observed near the assay signal, not to realize assay in whole blood samples.

In the following, we will demonstrate the feasibility of SERS tags in the whole blood samples. The Raman measurement of SERS tags and silica-coated SERS tags in whole blood and PBS buffer were executed with the excitation wavelength of 785 nm. Fig. 4 indicates the SERS spectra of the Ag@4-MBA and Ag@4-MBA@SiO<sub>2</sub> in PBS or whole blood measured after 10 min. In Fig. 4A, the SERS of Ag@4-MBA in the whole blood is far lower than that in water, and the peaks shift

toward higher wave-number, indicating that the Ag@4-MBA is not appropriate for applications in whole blood. The decrease of signal is ascribed to the reduction of concentration of SERS tags in whole blood because of the aggregation of the Ag@4-MBA in whole blood (Doering and Nie, 2003). The shift of SERS peak verifies that there appear the interfering molecules on the surface of the Ag NPs. In contrast to Ag@4-MBA, the intensity variation of Ag@4-MBA@SiO<sub>2</sub> is about 10%, and no peak shift appears. The decrease in intensity of Ag@4-MBA@SiO<sub>2</sub> is primarily ascribed to substantial scattering loss in the whole blood solutions, demonstrating that the homogeneous assay in whole blood is worth reconsidering.

Here, we use the optical fiber as the supporter of assay. At the same time, the fiber is used to transport the excitation light and detecting



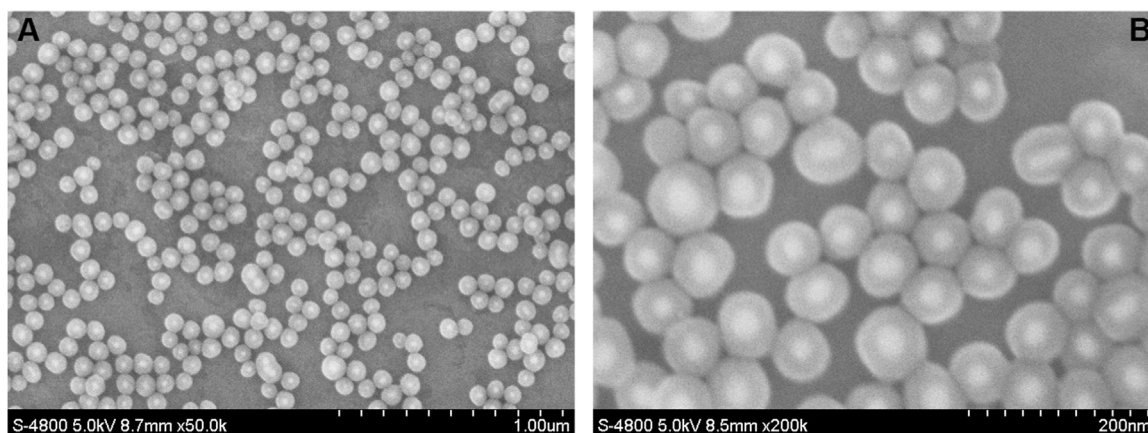


Fig. 2. FE-SEM of silica-coated SERS-tags (A), (B) is the corresponding higher magnification ratio.

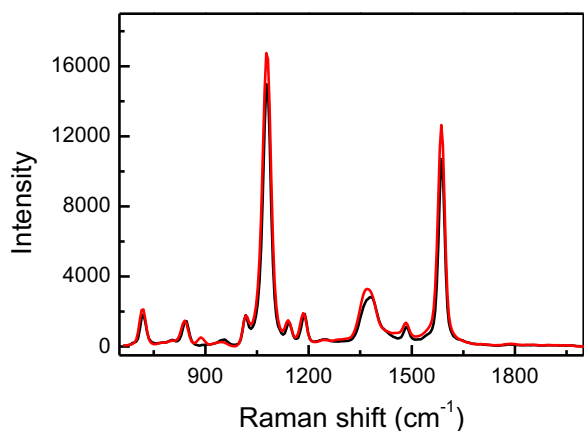


Fig. 3. SERS spectra of aqueous suspension of SERS tags before (black line) and after (red line) silica encapsulation. Both spectra were obtained with NIR laser excitation (785 nm). (For interpretation of the references to color in this figure legend, the reader is referred to the web version of this article.)

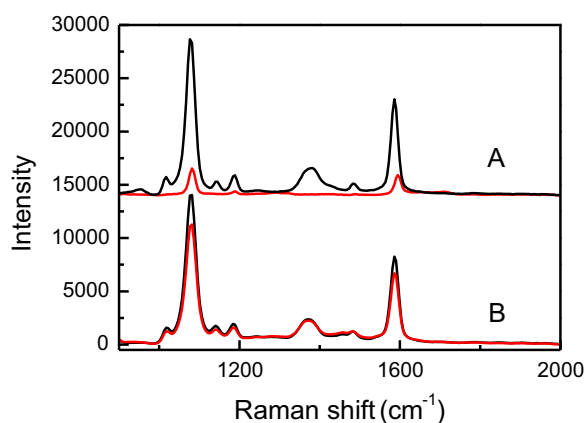


Fig. 4. SERS spectra of Ag@4-MBA (A) and Ag@4-MBA@SiO<sub>2</sub> (B) in water (black line) or whole blood (red line). Both spectra were obtained with 785 nm laser excitation. (For interpretation of the references to color in this figure legend, the reader is referred to the web version of this article.)

signal. Therefore, we studied the influence of the blood samples on the silica-coated SERS tags modified on the optical fiber. The measured spectra are shown in Fig. S4. The increase of signal is observed, attributed to the scattering of blood. Therefore, the method based on fiber is superior to homogeneous assay.

### 3.3. Protein detection in whole blood using optical fiber biosensor with Ag@4-MBA @SiO<sub>2</sub> as labels

The above results prove that the constructed silica-coated SERS tags is fit for the unprocessed whole blood samples, which triggered the initiative in this work of exploring the SERS tags to construct a FOB for *in situ* assay in whole blood with excitation wavelength of 785 nm.

Detection of biomarkers promises great potential for early diagnosis of related diseases. As a major plasma protein, AFP level in serum albumin is related to many diseases. For instance, AFP has been applied as a biomarker for monitoring hepatocellular carcinoma and a raised AFP level is often used in the clinical diagnosis of primary liver cancer (Schieving et al., 2014; Temelso et al., 2014). Until now, various methods have been used for the detection of AFP (Arya and Bhansali, 2011). However, few works have been done to detect AFP in whole blood *in situ*. In our study, SERS nano-tags integrated FOB was used to detect AFP in unprocessed blood samples. The principle is schematically shown in Fig. 1. AFP modified SERS tags are firstly bound on the side of fiber core through the interaction between rabbit anti-AFP and AFP, yielding a relatively high SERS signal. When the fiber is dipped into the detection solution with the presence of AFP, the AFP modified SERS tags are displaced from the side of fiber core by displacement reaction and leave the evanescent wave region, inducing a decrease in the SERS signal (Selinger and Rabbany, 1997). The change in value seriously relates with the concentration of AFP in the detection solution. Therefore, the SERS signal offers a rapid *in situ* detection of AFP in whole blood. The detection setup is shown in Fig. S5A. Calibration of the FOB was completed by applying the FOB with known concentrations of AFP dissolved in PBS and whole blood. Fig. 5 shows the AFP concentration dependent SERS signal ( $(I_0 - I)/I_0$ ) in PBS or whole blood samples. The  $I_0$  and  $I$  refer to the SERS signal with the Raman shift at 1076 cm<sup>-1</sup> without and with the AFP in the analyte solutions, respectively.

The change of SERS signal refers to the difference between the SERS signal in the absence and presence of AFP. The difference increases linearly with AFP concentrations between 50 and 500 ng/mL in whole blood samples. The coefficient of correlation ( $R^2$ ) was 0.98, showing a reasonable linear sensible range. But the linear range in PBS samples is from 20 to 300 ng/mL and the coefficient of correlation ( $R^2$ ) was 0.99. The limit of detection (LOD) for PBS and blood samples is 3 and 17 ng/mL, respectively. The discrepancy between PBS and whole blood maybe comes from the complex of whole blood, decreasing the reaction probability between rabbit anti-AFP and AFP (Liu et al., 2013). Further addition of BSA (0.01 mg/mL), or rabbit IgG (0.01 mg/mL) into the measured solution did not interfere with the SERS signal, showing a higher stability and specificity. The reproducibility of FOB assay was also estimated. The relative standard deviation for six detections of 500 ng/mL AFP was

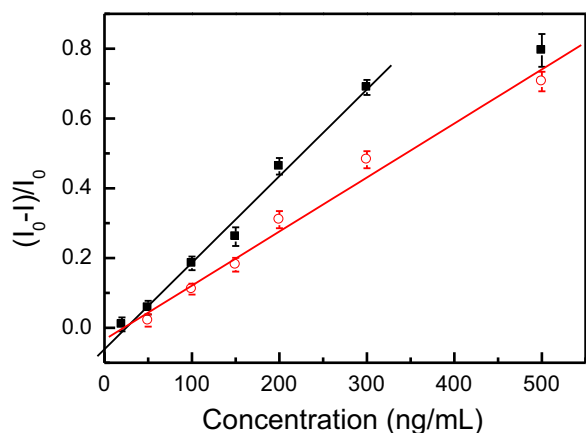


**Fig. 5.** The difference values of SERS signal at  $1076\text{ cm}^{-1}$  as varying concentration of AFP in PBS (black squares) and whole blood (red circles) solutions. (For interpretation of the references to color in this figure legend, the reader is referred to the web version of this article.)

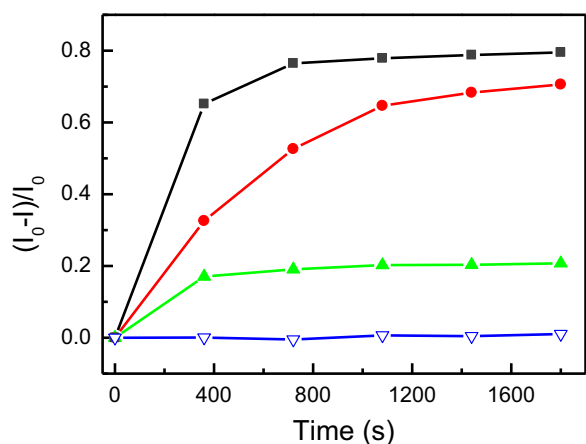


**Fig. 6.** The measured SERS signal at  $1076\text{ cm}^{-1}$  responses to the reaction time with the AFP in PBS (square), without (inverted triangle) and with the AFP (triangle) in the wistar rat, and the whole blood solution (circle) with the AFP concentration of  $500\text{ ng/mL}$ .

3%,

implying that FOB assay has great potential for the *in situ* detection of AFP in unprocessed whole blood samples, which avoids the need for complicated processing steps to separate serum or plasma and makes the point-of-care (POC) application of the FOB more likely.

As a proof-of-concept, we have *in vivo* and *in situ* monitored AFP in the whole blood of the wistar rat to seek the feasibility of *in vivo* application. Here, we injected AFP physiological saline solution into the wistar rat by jugular. The volume of the whole blood in the wistar rat was calculated based on the 8% of the rat weight. The experiment equipment is shown in Fig. S5B. However, it is difficult to obtain the feasible detecting results in the wistar rat. As well known, the FOB was not only used for assay as described above but also offered a powerful tool for monitoring protein interaction processes *in situ* and in real time, and thus could provide information on protein interaction kinetics. Therefore, we also used the FOB to dynamically observe the reaction process to try to reveal the origin of the discrepancy in different solutions: PBS, the whole blood and *in vivo*. The dynamic curves are shown in Fig. 6. The results demonstrate the association ability is the strongest in PBS solution. However, after 360 s, the association ability in whole blood is stronger than that in PBS. Comparing the whole blood with PBS, we think the complexity of blood composition blocks the interaction between rabbit anti-AFP and AFP. The association ability *in vivo* severely decreases with the whole blood before 360 s. Moreover after 360 s, the discrepancy remains

almost no changes. In the whole blood or *in vivo*, the difference of the blood composition comes from the blood anticoagulant that can not be enough to change their interaction. As well known, *in vivo* application of probes must insure sufficient biocompatibility. When the probes intact with blood, there appear an interface layer between the blood and probe, and present some unpredictable reactions. For example, the platelets, protein and blood cells are attached to the surface of the probes, and the blood clotting function of platelets is activated, forming a thrombus (Escobar and White, 2000). Therefore, we infer it is the unpredictable reaction *in vivo* that results in the association ability rapidly diminishes. In the subsequent work, we will concentrate on the biocompatibility of optical fiber probe to research the effect of biocompatibility on *in vivo* assay.

#### 4. Conclusions

This work focuses on how to construct an evanescent wave-based FOB using SERS nano-tag as label for direct detection in unprocessed whole blood. It is concluded that the  $\text{Ag}@4\text{-MBA}@SiO_2$  is an effective label for application in unprocessed blood by using the NIR laser-785 nm excitation. Combined with optical fibers, the influence of light scattering from the blood composition on the detecting signal is eliminated, superior to the homogeneous assay. Moreover, a new *in situ* immune assay of AFP in unprocessed whole blood was developed by using evanescent wave theory. The results demonstrate the constructed FOB holds sensitive and reproducible response to the AFP concentration in the range from 50 to  $500\text{ ng/mL}$  in unprocessed blood. Moreover, the dynamic observations of AFP in PBS and unprocessed blood samples prove the complicated composition seriously influenced the diffusion coefficient. Importantly, preliminary wistar rat experiment highlights that this method could be developed into a new assay method for *in vivo* and *in situ* analysis.

#### Acknowledgements

This work was supported by the National Natural Science Foundation of China (11374297, 61071048, 21405149 and 11604331), and exchange program between CAS of China and KNAW of the Netherlands, IOP program of the Netherlands and John van Geuns foundation.

#### Appendix A. Supplementary material

Supplementary data associated with this article can be found in the online version at <http://dx.doi.org/10.1016/j.bios.2016.10.070>.

#### References

- Arppe, R., Mattsson, L., Korpi, K., Blom, S., Wang, Q., Riittamäki, T., Soukka, T., 2015. Anal. Chem. 87, 1782–1788.
- Arya, S.K., Bhansali, S., 2011. Chem. Rev. 111, 6783–6809.
- Bishnoi, S.W., Rozell, C.J., Levin, C.S., Gheith, M.K., Johnson, B.R., Johnson, D.H., Halas, N.J., 2006. Nano Lett. 6, 1687–1692.
- Bosch, M.E., Sanchez, A.J.R., Rojas, F.S., Ojeda, C.B., 2007. Sensors 7, 797–859.
- Doering, W.E., Nie, S.M., 2003. Anal. Chem. 75, 6171–6176.
- Escobar, G., White, J.G., 2000. Thromb. Haemost. 83, 371–386.
- Kong, X.M., Yu, Q., Zhang, X.F., Du, X.Z., Gong, H., Jiang, H., 2012. J. Mater. Chem. 22, 7767–7774.
- Leung, A., Shankar, P.M., Mutharasan, R., 2007. Sens. Actuators B 125, 688–703.
- Li, L., Ding, H.Y., Di, B., Li, W.L., Chen, J., 2012. Analyst 137, 5632–5638.
- Liu, Y., Zhou, Q., Revzin, A., 2013. Analyst 138, 4321–4326.
- Nie, S.M., Emory, S.R., 1997. Science 275, 1102–1106.
- Pansare, V.J., Hejazi, S., Faenza, W.J., Prud'homme, R.K., 2012. Chem. Mater. 24, 812–827.
- Scarabelli, L., Coronada-Puchau, M., Giner-Casares, J.J., Langer, J., Liz-Marzan, L.M., 2014. ACS Nano 8, 5833–5842.
- Schieving, J.H., Vries, M., de Vugt, J.M.G., Weemaes, C., Deuren, M., van Nicolai, J., Wevers, R.A., Willemsen, M.A., 2014. Eur. J. Paediatr. Neurol. 18, 243–248.
- Selinger, J.V., Rabbany, S.Y., 1997. Anal. Chem. 69, 170–174.
- Sha, M.Y., Xu, H.X., Natan, M.J., Cromer, R., 2008. J. Am. Chem. Soc. 130, 17214–17215.

- Sun, C., Chen, L.B., Xu, F.J., Zhu, P.Y., Luan, J.F., Mao, C., Shen, J., 2013. J. Mater. Chem. B 1, 801–809.
- Taitt, C.R., Anderson, G.P., Ligler, F.S., 2005. Biosens. Bioelectr. 20, 2470–2487.
- Temelso, B., Alser, K.A., Gauthier, A., Palmer, A.K., Shields, G.C., 2014. J. Phys. Chem. B 118, 4514–4526.
- Wang, X.D., Wolfbeis, O.S., 2013. Anal. Chem. 85, 487–508.
- Wang, Y.Q., Yan, B., Chen, L.X., 2013. Chem. Rev. 113, 1391–1428.
- Wencel, D., Abel, T., McDonagh, C., 2014. Anal. Chem. 86, 15–29.
- Xie, L.X., Qin, Y., Chen, H.Y., 2013. Anal. Chem. 85, 2617–2622.
- You, L., Mao, Y.W., Ge, J.P., 2012. J. Phys. Chem. C 116, 10753–10759.
- Zhang, Y.L., Li, X.K., Xue, B., Kong, X.G., Liu, X.M., Tu, L.P., Chang, Y.L., 2015. Sci. Rep. 5, 14934.
- Zhang, Y.L., Zeng, Q.H., Sun, Y.J., Liu, X.M., Tu, L.P., Kong, X.G., Buma, W.J., Zhang, H., 2010. Biosens. Bioelectron. 26, 149–154.